

Investigation in to Properties of Polyurethane Closed Cell by High Loading of SiO₂ Nanoparticles

M. Nadafan¹, R. Malekfar^{1*} and Z. Dehghani²

1- Department of Physics, Tarbiat Modares University, Tehran, I. R. Iran.

2- Department of Physics, Faculty of Basic Sciences, University of Neyshabur, Neyshabur, I. R. Iran.

(*). Corresponding author: malekfar@modares.ac.ir

(Received: 08 July 2014 and Accepted: 05 Sep. 2015)

Abstract

In this research the composition of polyurethane closed cell (PUCC) with two different concentrations of SiO₂ nanoparticles (1.0 and 2.0 wt%) have been prepared. Optical microscopy and SEM imaging, watering uptake, FTIR and Raman spectroscopy of the synthesized samples were carried out. The optical microscopy imaging of samples showed differences in the appearance of matrix produced by applying different concentrations of SiO₂ nanoparticles (NPs). The mean cell size of the foams decreased with the addition of SiO₂ NPs from 0.0 wt% up to 2.0wt%. Variation in the water uptake of specimens is related to the function of SiO₂NPs concentrations. The degree of phase separation and the hydrogen bonding index in samples were evaluated in terms of their FTIR spectroscopy data. The apparent and real densities of foams were measured and then total, open and closed porosity of samples were calculated. With elevating the amount of nanoparticles the open porosity of samples almost increased, while the closed and total porosity decreased. The Raman spectra of the synthesized samples were used for evaluating possible interaction between SiO₂ NPs and PUCC foams.

Keywords: FTIR, Polyurethane, Raman Spectroscopy, Silica.

1. INTRODUCTION

Polyurethanes (PUs) are kinds of attractive synthetic materials in industry that are widely used in coating, synthesizing and preparing leathers, fibers, foams, thermoplastic elastomers and so on [1-3]. Nowadays, scientists like to produce PU with high performance by changing some factors that affect the morphology of PU such as the hard and soft sections of the PU matrix, size and weight of these two components and chemical construction of the chains of PU. Furthermore, lack of having important properties of organic polymers such as stability at low temperature and weak mechanical aspects has led to entrance inorganic materials for

improving organic matrices. Organic–inorganic composite materials have both advantages of organic polymers and inorganic materials including flexibility, ductility, rigidity and high thermal stability that come from both of inorganic and organic agents [4].

Silica nanoparticle (NP) is one of the porous inorganic materials with high specific surface area and high surface energy. The researchers have shown that silica is useful for improving polymer matrix especially in mechanical–thermal–chemical properties [3]. In this research we have tried to evaluate the influence of the presence of silica in PU matrix with

considering some properties. Some aspects such as watering uptake, real and apparent density, porosity of synthesized samples were evaluated.

Furthermore, the interaction between silica and polyurethane was analyzed by FTIR and Raman spectroscopy.

However, optical microscopy and SEM imaging could help to understand how silica can alter morphological structure of synthesized foams.

2. MATERIAL AND METHODS

Silicon Oxide NP (99.5 %, S-type, Spherical particles, 15–20 nm, amorphous) was purchased from US Research Nanomaterials, Inc. Diphenylmethane diisocyanate (MDI, density=1.23g/cm³), polyether polyol (RCC: Rigid Closed Cell, density=1.1g/cm³) surfactant, catalyst and blowing agent (HCF-C) were prepared from Exxon Panah Co., Ltd., Tehran, I.R, Iran.

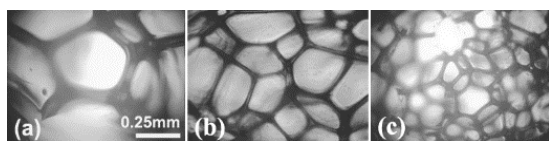


Figure 1. Optical micrographs of the PUCF foams with SiO₂ NPs content of (a) 0.0 wt. %, (b) 1.0 wt. %, and (c) 2.0 wt. %.

2.1. Preparation of PUCF/SiO₂

Appropriate amounts of silica (1-2 wt%) were dissolved into closed cell polyol part by using an electrical MS2 Minishaker IKA (Germany). This lasted for 20 seconds with 3000 rpm until a homogenized solution was obtained. Then, the MDI part was added to the prepared solution by vortex mixing under 2000rpm for 4–5 seconds. Due to well-prepared sample and producing CO₂ gas during reaction time, the cover of the container of polyurethane closed cell (PUCF)/SiO₂ was taken off. After 10–12 seconds, reaction was completed by forming of foams with the equal ratio of polyol: MDI. For characterization purposes, thin pieces of

samples with 1mm diameter were cut and soaked up into liquid nitrogen to prepare freezing samples for further analysis.

3. RESULTS AND DISCUSSION

3.1. Microscopic Evaluation

In order to determine cell size of PUCF and observing its microstructure, optical microscopy is used. For this aim, thin layers of blank PUCF and PUCF/SiO₂ nanocomposite with thicknesses of about 1mm were cut perpendicular to the rising direction of foam. The freeze-fractured surfaces of all samples were obtained at liquid nitrogen temperature and then were examined.

It can be seen in Figure. 1 that by increasing of SiO₂ NPs in pure PUCF the mean cell sizes in the matrix have decreased in comparison with pure PUCF. This finding is reasonable because silica can fill the empty spaces and bring the cells close together. Accordingly, by increasing SiO₂ NPs in pure PUCF the mean cell sizes in the matrix have decreased. The average cell sizes consequently changed from blank samples (720±430), PUCF/1 wt% SiO₂ (700±180) to PUCF/2 wt% SiO₂ (570±85).

3.2. SEM Analysis

The exact microstructural features of the synthesized samples were characterised by image analysis of foam's sections. The synthesized samples were analysed under a SEM, Seron Technology-AIS2100 model, using 30 kV accelerating voltage after coating the samples with a thin layer of gold. All foam pictures were taken perpendicular to the foam rising direction. SEM images confirmed the given results from optical micrographs. The cell sizes were determined more exactly by SEM than optical imaging. It is clear in Figure. 2 that by adding SiO₂ NPs from 0.0 wt% to 2.0 wt% into PUCF, the average cell size is finer. Obtained samples were analyzed by SEM at different magnifications. Here,

only the SEM images of nanocomposite foams with SiO₂ NPs contents of 1.0 wt% are shown in Figure. 3. As it is seen in Figures. 3(a)–3(e), closed inspection (with $\times 100$, $\times 500$, $\times 1.0k$, and $\times 6k$ and $\times 30k$ magnifications, respectively) of the cell struts reveals that the PUCC/SiO₂ nanocomposite foams have micro-porous skeleton. The presence of the micro voids can be due to the chemical reactivity of SiO₂ NPs with the isocyanate monomer [5]. Presence of SiO₂ NPs in micro void of PUCC/SiO₂ nanocomposite foams gives evidence on the mentioned claim.

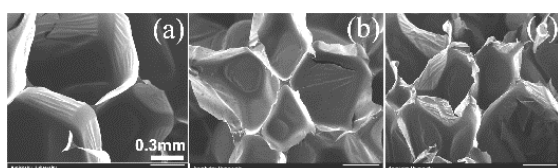


Figure2. SEM images of the PUCC foams with (a) 0.0 wt. %, (b) 1.0 wt. %, and (c) 2.0 wt. %, SiO₂ NPs.

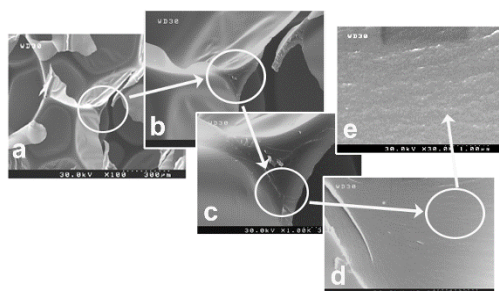


Figure3. SEM images of PUCC nanocomposite loaded with 1.0 wt% SiO₂ NPs at different magnification, (a) $\times 100$, (b) $\times 500$, (c) $\times 1k$, (d) $\times 6k$ and (e) $\times 30k$ to show micro voids.

3.3. Back-scattering raman analysis

Raman spectra of the samples were collected by using a Thermo Nicolet Almega dispersive micro-Raman spectrometer operating by a 532 nm laser line as the second harmonic of an Nd: YLF laser in a back-scattering configuration. The Raman spectra of the synthesized samples (Figure.4) were used for

evaluating possible interaction between SiO₂ NPs and PUCC foams. It can be seen that by adding SiO₂ NPs to PUCC matrix the C–H wagging bond at 850 cm⁻¹ has been appeared stronger [6]. This peak was shifted toward lower wave numbers by increasing the amount of SiO₂ NPs in PUCC matrix. The Raman peaks at 626 cm⁻¹ [6], 760 cm⁻¹ [7] and 1045 cm⁻¹ [8] are assigned as the C–C–C bending mode, Si–O bending and Si–O–Si stretching vibration bond, respectively, that are just in PUCC/SiO₂ samples but more SiO₂ into PUCC matrix causes more shift toward higher wave-numbers. All the synthesized samples have C–C stretching bond at around 1590 cm⁻¹ [6] and by adding SiO₂ NPs to pure PUCC the intensity of this peak starts to increase.

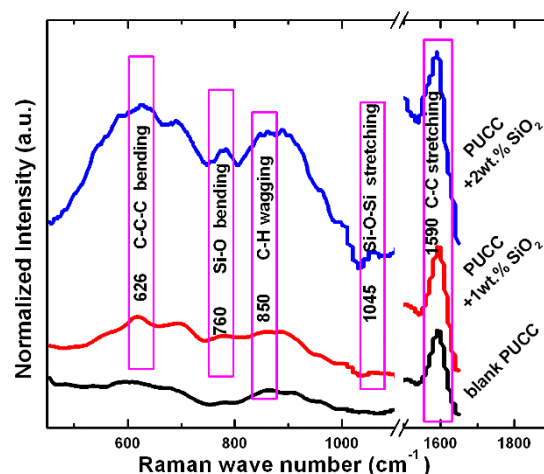


Figure4. Raman spectra of blank PUCC, and PUCC/SiO₂ nanocomposites.

3.4. FTIR spectroscopy analysis

Fourier transform infra-red (FTIR) transmission spectra of the samples as powder-pressed KBr pellets were collected using a Thermo Nicolet Nexus 670 FTIR spectrometer system with 4 cm⁻¹ resolution and in the wave-number range from 4000 to 400 cm⁻¹ at room temperature.

The synthesized PU samples were characterized using FTIR spectroscopy. The FTIR spectra came from the PUCC/SiO₂ over the frequency range of 4000–400cm⁻¹ are shown in Figure. 5. By

comparing the three FTIR spectra, most of their absorption peaks were similar and some of them were related to existence of SiO₂ and its interaction with PUCC. The intensity of peaks at 702 [9] and 1130 cm⁻¹ [10] in Figure. 5 are assigned to Si-C and Si-O-Si, respectively. By rising SiO₂ NPs at 2.0 wt% the intensity of the mentioned peaks increases. The symmetric Si-O-Si stretching bond at 755 and 795 cm⁻¹ are related to extra amount of SiO₂ NPs into PUCC [9].

The FTIR spectrum of PUCC nanocomposite shows that the intensity of peak at 1450 cm⁻¹ is related to the reactions between isocyanate and urethane groups as a secondary reaction. The intensity of this peak in PUCC nanocomposite foams was higher than blank PUCC [11]. Probably, the SiO₂ NPs causes extra cross linking sites. The other peaks such as 1530 and 3351 cm⁻¹ in Figure. 5 are assigned to N-H bending [12] and N-H bonds of urethane [13]. The intensity of these peaks were decreased in SiO₂ NPs to 1.0 wt%, and afterward it start to increase up to 2.0 wt%.

An important factor which can be achieved from the FTIR spectroscopy data is the degree of phase separation which is one of the fundamental factors for evaluating physical properties of PUCC foam. Xia and Song [14] investigated the degree of phase separation (DPS) by the Cooper method. There are two main types of hydrogen bonds in PU: hydrogen bonding and free carbonyl group. The relative amounts of the two types of hydrogen bonds are determined by DPS. An increase in this separation favours the inter-urethane hydrogen bonds. The degree of hydrogen bonding of the carbonyl groups can be studied by examining the carbonyl stretching region of the spectrum. The two bonded and free carbonyl groups [15] are associated to the peaks at about 1700 and 1720 cm⁻¹, respectively, which play a main role in determining DPS factor.

The hydrogen bonding index, R, is introduced as $R = A_{bonded} / A_{free}$, where the

$A_{bonded} = 1 - T_{bonded}$ and $A_{free} = 1 - T_{free}$ are the absorbance peak intensity of 1700 and 1720 cm⁻¹ carbonyl groups, respectively. Furthermore, DPS is given by the following equation: $DPS = R / (R + 1)$. The increase in R factor in PUCC/SiO₂ nanocomposites is referred to the dispersion of silica NPs into the soft segments of the polymer by means of a hydrogen bonding between the silica and polyol hydroxyl groups and other groups of the polyol in PUCC [16].

According to 1700 cm⁻¹, the bond carbonyl groups wave-number and 1720 cm⁻¹, the free carbonyl groups wave-number, the hydrogen bonding index, R, and DPS decrease for the samples with doping of up to 1.0 wt% SiO₂ contents and start to increase for the doping of up to 2.0 wt% SiO₂ NPs (Table1). As it was mentioned, the silica NPs have tendency to disperse in hard segments of PUCC/1.0 wt% SiO₂ but by increasing the amount of SiO₂ NPs, they prefer to disperse in the soft segments of the structure.

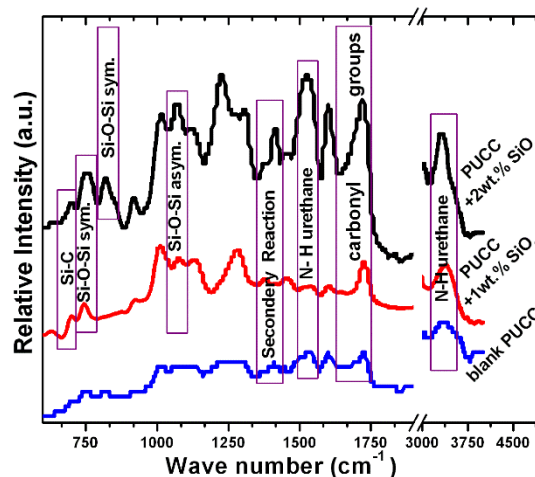


Figure 5. FTIR spectra of blank PUCC and PUCC/SiO₂ nanocomposites

3.5. Water uptake

In order to determine the water uptake and water absorption of the samples, all samples were cut to 10mm × 10mm dimensions with 1mm thickness. The samples were dried in a vacuum oven for

24 hours and their dry weights were measured as W_d . The wet weight of soaking samples (W_t) was examined in deionized water at room temperature at different immersion times up to 96 hours. Water absorption of the samples was calculated using the following equation [17]:

$$W(\%) = \{(W_t - W_d) / W_d\} \times 100 \quad (1)$$

The mean of three different readings was taken.

Figure 6 shows the water absorption of PUCC/SiO₂ NPs. As it was seen the composites of PUCC were achieved to saturated state for water uptake in about first twenty hours. The most water up taking of PUCC samples is related to the samples with amounts of 2.0 wt% SiO₂ NPs in polymer matrix. Water uptake of samples with SiO₂ NPs is higher than pure samples; this is reasonable for the inherent hydrophilic of SiO₂NPs. The results show that the maximum amount of water up taking in samples including SiO₂ nanoparticles was about 12 times related to the blank sample.

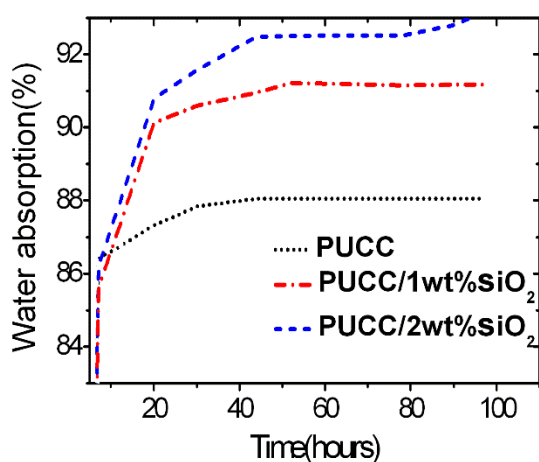


Figure 6. Water absorption of PUCC/SiO₂ NP.

3.6. Apparent density and real density

For obtaining apparent and real density, three various specimens were cut from different regions of the prepared foams and

the average values of the densities were measured. The apparent density (bulk density) is done by division of the masses by the related volumes which have the dimension of kg/m³ or gr/cm³. A common way to measure the bulk density of a porous material is based on Archimedes 'principle, by hydrostatic balance and immersing of samples in the water.

Figure 7 indicates the apparent density of PUCC foams versus the SiO₂ NP loading segments. By adding filler into blank PUCC, the apparent density increases at higher loading segments. By increasing apparent density of sample, the mean cell sizes reduced. This can be understood from the optical microscopy and SEM images as well. However, by adding SiO₂ NPs up to 2.0 wt% concentration, the apparent density increased much more than blank PUCC sample.

The real density of the samples were measured by immersing them and recording the water displacement (pycnometry) as it introduced the ratio of its mass to the volume enclosed by an envelope of water surrounding the foam [18]. The real density of PUCC foams versus the SiO₂ NPs loading fractions are seen in Figure. 7.

When the mean cell size of the foams increased, the real density of the foams decreased; which is probably related to the higher mass in the same volume. As it can be seen, the real density of PU is higher than the apparent density of it due to the presence of micro voids in the structure. It can be understood that the amount of NPs is an important factor in water absorption and determining the density of the samples.

3.7. Porosity

As it was mentioned during chemical reaction of producing foams, the blowing agent causes the micro voids in the cell strut that takes a role in determination and construction of porosity. The fraction of the total volume that is non-occupied is

porosity [19]. Having higher open porosity is a good hint for being a better sound absorber. Figure 8 shows the total porosity, open porosity and closed porosity of the PUCC samples versus the SiO₂ NPs loading fractions.

By using the following equation, the percentage of the total porosity of the prepared samples was measured according to the following equation [20].

$$\varphi_{total} = (1 - \rho_{apparent} / \rho_{real}) \times 100\% \quad (2)$$

The real and apparent densities of the samples were measured in previous section. When the amount of SiO₂ NPs increased up to 2.0 wt% and the total porosity decreased.

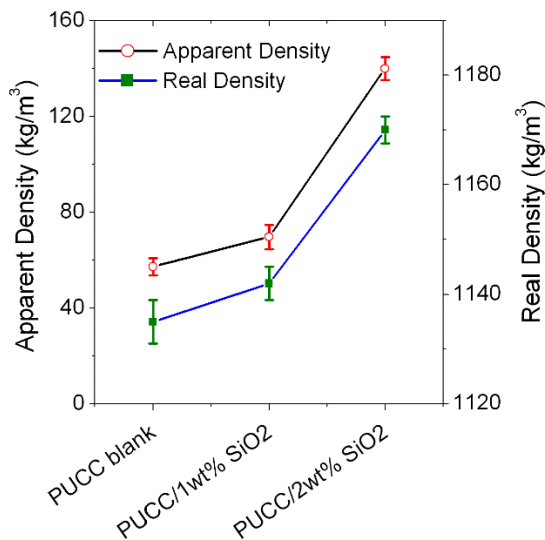


Figure 7. Apparent and real density of blank PUCC and PUCC/SiO₂ NPs.

On the other hand, the open porosity is a sign of sound absorption that the foam with high open porosity is a good sound absorber [21]. Considering the given data from water absorption and also the saturation time of samples, the volume of water was measured using the following equation:

$$V_{water} = (m_{saturated} - m_{dry}) / \rho_{water} \quad (3)$$

Where $m_{saturated}$ is the mass of water saturated foam and m_{dry} is the dry mass of samples after taking it out of the oven. ρ_{water} is the mass density of water. If the V_{water} is divided by the original foam volume, the percentage of open porosity of samples is obtained, and the difference between the percentage of open porosity and total porosity is the percentage of closed porosity of samples.

In PUCC nanocomposites by increasing the SiO₂ NPs up to 2.0 wt%, the open porosity of PUCC nanocomposites approximately increases. Furthermore, by decreasing cell sizes of the samples the open porosity increases, because decreasing of mean cell size tends to higher conductivity of water into samples and causes more water absorption by them.

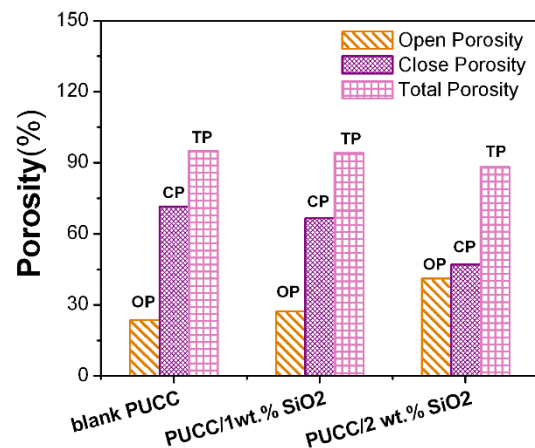


Figure 8. Total porosity, open porosity and closed porosity of blank PUCC and PUCC/SiO₂ NPs.

4. CONCLUSIONS

Two PU hybrids with SiO₂ NPs were prepared by using in situ polymerization method. Also, the relationship between the mentioned foam microstructure via SEM and its different optical and mechanical properties were investigated. The interaction between PU matrix and SiO₂ NPs and thus the effects of this interaction on mentioned properties of PUCC/SiO₂ nanocomposites were examined through

Raman and FTIR spectra. The following points can be concluded:

- The mean cell sizes of the foams decreased with the addition of SiO₂ NPs from 0.0wt% up to 2.0wt%.

- The presence of SiO₂ NPs in a micro void of PUCC/SiO₂ nanocomposite foams gives evidence on the claim that the reaction between SiO₂ NPs, polyol part and the CO₂ gas production leads to create micro voids in the foam.

- The results indicate that there is maximum 15% increase in the apparent density of PUCC/SiO₂ nanocomposite foams in comparison with the blank PUCC foam.

- The real density reached a maximum up to about 3.1% higher than the blank PUCC foam for 2.0 wt% of loading fraction.

- The open porosity of the PUCC nanocomposite foam reached a maximum up to about 74% higher than the blank PUCC foam for 2.0wt% of SiO₂ content.

- The water absorption of samples has shown the PUCC/2.0 wt% SiO₂ NPs was the best sample considering water absorption.

- The open porosity of PUCC was twice the blank PUCC by increasing SiO₂ NPs up to 2.0 wt%. This feature is important for constructions used in civil engineering and as a source of sound insulator.

REFERENCES

1. B. Yildiz, M. O. Seydibeyoglu and F. S. Guner: *Polym. Degrad. Stab.*, Vol. 94, (2009), pp. 1072-1075.
2. L. Bisticic, G. Baranovic, M. Leskovic and E. G. Bajsic: *Eur. Polym. J.*, Vol. 46, (2010), pp. 1975-1987.
3. Y. Zhu, X. Zhao, Z. Wang, D. An, Y. Ma, S. Guan, Y. Du, B. Zhou and X. Gao: *Appl. Surf. Sci.*, Vol. 257, (2011), pp. 4719-4724.
4. S. Pandey and S. B. Mishra: *J. Sol-Gel Sci. Technol.*, Vol. 59, (2011), pp. 73-94.
5. M. Bandarian, A. Shojaei and A. M. Rashidi: *Polym. Int.*, Vol. 60, (2011), pp. 475-482.
6. O. M. Primera-Pedrozo, G. D. M. Rodriguez, J. Castellanos, H. Felix-Rivera, O. Resto and S. P. Hernandez-Rivera: *Spectrochim. Acta A Mol. Biomol. Spectrosc.*, Vol. 87, (2012), pp. 77-85.
7. E. R. Jisha, G. Balamurugan, P. Selvakumar, N. Edison and R. Rathiga, *Int. J. Pharm Tech Res.*, Vol. 4, (2012), pp. 1323-1331.
8. M. Gnyba, M. Jedrzejewska-Szczerska, M. Keranen and J. Suhonen, *Proc., XVII IMEKO World Congress, Dubrovnik, Croatia, (2003)*. pp. 237-240.
9. H. Zhou, Y. Chen, H. Fan, H. Shi, Z. Luo and B. Shi: *J. Memb. Sci.*, Vol. 318, (2008), pp. 71-78.
10. Z. Wang, Y. Zhou, Q. Yao and Y. Sun: *Appl. Surf. Sci.*, Vol. 256, (2009), pp. 1404-1408.
11. J. L. Rivera-Armenta, T. Heinze and A. M. Mendoza-Martinez: *Eur. Polym. J.*, Vol. 40, (2004), pp. 2803-2812.
12. S. Parnell, K. Min and M. Cakmak: *Polym.*, Vol. 44, (2003), pp. 5137-5144.
13. R. C. S. Araujo, V. M. D. Pasa and B. N. Melo: *Eur. Polym. J.*, Vol. 41, (2005), pp. 1420-1428.
14. H. Xia and M. Song, *Soft Matter*, Vol. 1, (2005), pp. 386-394.
15. L. Bisticic, G. Baranovic, M. Leskovic and E. G. Bajsic: *Eur. Polym. J.*, Vol. 46, (2010), pp. 1975-1987.

16. M. A. Semsarzadeh and B. Ghalei: *J. Memb. Sci.*, Vol. 432, (2013), pp. 115-125.
17. C. Y. Bai, X. Y. Zhang, J. B. Dai and C. Y. Zhang: *Prog. Org. Coating.*, Vol. 59, (2007), pp. 331-336.
18. J. Rouquerolt, D. Avnir, C. W. Fairbridge, D. H. Everett, J. H. Haynes, N. Pernicone, J. D. F. Ramsay, K. S. W. Sing and K. K. Unger: *Pure & Appl. Chem.*, Vol. 66, (1994), pp. 1739-1758.
19. C. Torres-Sanchez and J. R. Corney: *Ultrason. Sonochem.*, Vol. 15, (2008), pp. 408-415.
20. J. L. Ryszkowska, M. Auguscik, A. Sheikh and A. R. Boccaccini: *Compos. Sci. Technol.*, Vol. 70, (2010), pp. 1894-1908.
21. S. Basirjafari, R. Malekfar and S. Esmailzadeh Khadem: *J. Appl. Phys.*, Vol. 112, (2012), pp. 104312-10432